Geotechnical Aspects of Underground Construction in Soft Ground – Zhou, Guan & Li (eds)

Improved determination of the constrained modulus in soft soils using the flat dilatometer test

S. Oberhollenzer
Norwegian Geotechnical Institute, Oslo, Norway
Institute of Soil Mechanics, Foundation Engineering and Computational Geotechnics, Graz University of Technology, Graz, Austria

L. Hauser, R. Marte, F. Tschuchnigg & H.F. Schweiger
Institute of Soil Mechanics, Foundation Engineering and Computational Geotechnics, Graz University of Technology, Graz, Austria

E.J. Lande
Norwegian Geotechnical Institute, Oslo, Norway

ABSTRACT: A wide range of geotechnical tasks demand a reliable determination of soil stiffness. Since undisturbed soil sampling is required but difficult for laboratory testing, parameter identification based on in-situ testing in combination with correlations have become more popular. Flat dilatometer testing (DMT) considers the penetration of a steel blade, equipped with a circular, expandable membrane, into the ground. The penetration process is usually stopped in 20 cm intervals for total stress measurements at defined membrane expansions. The present article aims to improve the determination of the in-situ constrained modulus in soft soils by means of DMT. Existing correlations are compared with oedometer results for Alpine deposits. It is shown that constrained moduli, derived from existing correlations, underestimate laboratory results, even when DMT readings are corrected for partial drainage effects. New correlations are developed to reach a better agreement between in-situ and laboratory results in fine-grained soils.

1 INTRODUCTION

Soft soils define the soil layering of various urban areas (e.g., Oslo, Mexico City, Ho Chi Minh) and represent challenging ground conditions due to their moderate stiffness and strength. Alpine regions in Austria are often characterized by several basins, formed during glacial periods and filled by mainly fine-grained sediments after the melting process of glaciers (van Husen 1979). These (geologically) young sediments are usually normally consolidated and high groundwater tables are present. Nowadays, touristic areas like Salzburg, Rosenheim or Bregenz are situated on top of such fine-grained deposits. Recordings confirm that insufficient parameter identification in combination with inappropriate construction measures have often led to building damages (e.g., tilting; cracks along the foundation and walls). Since sampling disturbance can strongly influence the laboratory results, in-situ tests such as the piezocone penetration test (CPTu) and the seismic flat dilatometer test (SDMT) are becoming increasingly popular for identifying soil parameters (Schnaid 2009). However, correlations proposed in literature are usually site-specific and cannot be generally applied. Therefore, Graz University of Technology in cooperation with the Federal Chamber of Architects and Chartered Engineering Consultants initiated the research project PITS (parameter identification using in-situ tests in silty soils) to allow an improved characterization of the stress-strain behavior in postglacial Alpine deposits (Oberhollenzer & Hauser 2022).

DOI: 10.1201/9781003413790-13

The present paper aims to improve the determination of the in-situ constrained modulus (M) in postglacial, Alpine deposits using DMT. Therefore, in-situ testing and soil sampling were performed at four test sites, namely *Rhesi*, *Lokalbahn Salzburg*, *Seekirchen* and *water reservoir Raggal*. Alternative DMT-testing procedures were further executed to consider for partial drainage effects (Oberhollenzer et al. 2023). Constrained moduli, derived from oedometer tests and flat dilatometer results (using corrected and uncorrected in-situ readings) are compared in the first step. Subsequently, new correlations are proposed for DMT to reach an improved agreement between in-situ and laboratory results in Alpine deposits.

2 METHODS

2.1 *DMT-equipment and test execution*

Piezocone penetration tests (CPTu) and seismic flat dilatometer tests (SDMT) were executed according to ISO 22476-1 and ISO 22476-11 at the test sites *Rhesi*, *Lokalbahn Salzburg*, *Seekirchen* and *water reservior Raggal*. A steel blade, containing a thin, expandable, circular steel membrane, is pushed into the soil during DMT execution (see Figure 1a). At regular intervals (of usually 20 cm) the penetration is stopped for consecutive pressure readings at defined membrane expansions. The standard procedure, namely DMT-STD, is summarized in the following:

- A-reading: pressure required to lift-off the membrane, approx. 15 seconds after reaching the testing depth.
- B-reading: pressure required to expand the membrane center about 1.1 mm, approx. 15 seconds after the A reading.
- C-reading (optional): pressure reading in A position after slowly deflating the membrane from position B.

When using the DMT-system developed by Marchetti (1980) the membrane is expanded pneumatically by the operator using a control unit. In contrast, the Medusa flat dilatometer test (Medusa DMT) enables a fully automated, hydraulic expansion of the circular membrane using a motorized syringe (Marchetti et al. 2018). The required pressure for expanding the membrane is measured by a high-accuracy transducer. An electric cable, running through the

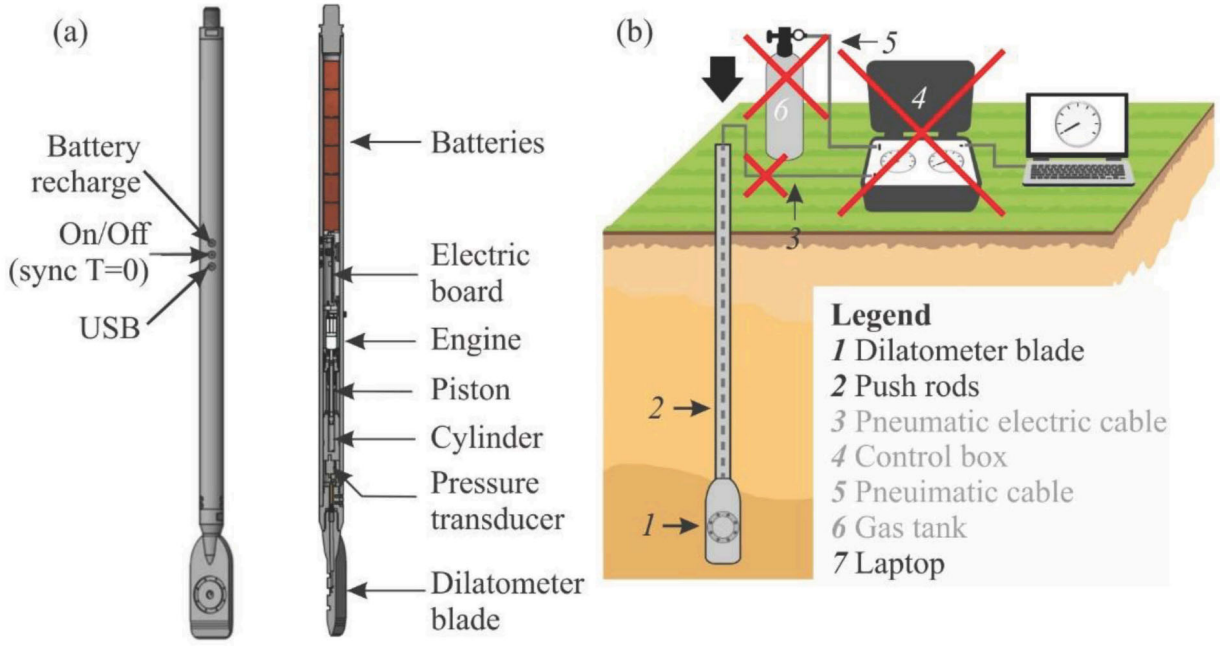

Figure 1. Overview of (a) DMT blade and the (b) components required for medusa test execution (Oberhollenzer et al. 2023).

penetration rods, is used instead of pneumatic cables during Medusa DMT execution connecting the blade with a control unit and the laptop for real-time data interpretation (see Figure 1b). Different membrane expansion rates and repeated A-readings (where the membrane is kept in the same position for repeated pressure readings) can be executed with high accuracy, enabling the enhanced testing procedure DMT-RA. The latter procedure considers repeated A-readings within the first 15 seconds after penetration stop, followed by B and C readings at the time-steps defined for DMT-STD. While DMT-STD were executed at the test sites *Rhesi* (depth: -25 m), *Lokalbahn Salzburg* (depth: 25 m), *Seekirchen* (depth: 12 m) and *water reservoir Raggal* (depth: 17 m), additional *DMT-RA* were considered at *Rhesi* and *Lokalbahn Salzburg*.

2.2 *DMT-interpretation*

The in-situ readings A, B and C are corrected about the membrane stiffness using the calibration offsets ΔA and ΔB according to Eq. (1), Eq. (2) and Eq. (3) (Marchetti 1980). Subsequently, corrected readings p_0, p_1 and p_2 are used to derive intermediate parameters, namely material index (I_D, see Eq. (4)), horizontal stress index (K_D, see Eq. (5)), dilatometer modulus (E_D, see Eq. (6)) and pore pressure index (U_D, see Eq. (7)), which represent the foundation for parameter identification according to Marchetti (1980). The in-situ constrained modulus (M) is calculated according to Eq. (8) using the dilatometer modulus (E_D) and the empirical factor R_M. For fine-grained soils characterized by $I_D \leq 0.6$, R_M should be calculated based on Eq. (9) but must be larger than 0.85 (Marchetti 1980).

$$p_0 = 1.05 \cdot (A + \Delta A) - 0.05 \cdot (B - \Delta B) \tag{1}$$

$$p_1 = B - \Delta B \tag{2}$$

$$p_2 = C + \Delta \mathrm{A} \tag{3}$$

$$I_D = (p_1 - p_0)/(p_0 - u_0) \tag{4}$$

$$K_D = (p_0 - u_0)/\sigma'_{v0} \tag{5}$$

$$E_D = 34.7(p_1 - p_0) \tag{6}$$

$$U_D = (p_2 - u_0)/(p_0 - u_0) \tag{7}$$

$$M = R_M \cdot E_D \tag{8}$$

$$R_M = 0.14 + 2.36 \cdot \log K_D \ (\mathrm{for} I_D \ \leq 0.6) \tag{9}$$

2.3 *Correction of DMT-readings about partial drainage effects*

Partial drainage effects can occur during DMT execution in a wide range of soil types (e.g., clays and silts) and are further influenced by soil heterogeneity (Oberhollenzer et al. 2023). Different researchers (e.g., Marchetti et al. 2001, Schnaid et al. 2018, Oberhollenzer et al. 2023) proposed test procedures to correct in-situ measurements for partial drainage, enabling a determination of undrained A- and B-readings (A0, B0) in the respective testing depth. It was previously shown that the in-situ readings show an approximately linear decrease over the root of time when keeping the membrane position fixed (see black dashed lines in Figure 2). The inclination of both lines is indicated as k_A and k_B. A- and B-readings, determined by means of DMT-STD, are indicated in Figure 2 by black circles.

It was recommended by Oberhollenzer et al. (2023) to determine undrained readings based on repeated A- and B-readings. The latter procedure is shown in green (see Figure 2) and consists of three main stages: (1) repeated A-reading within the first 15 seconds after penetration

stop (A0 → A15), (2) membrane expansion to position B and (3) repeated B-readings for 15 seconds (B30 → B45). While A0 is measured, B0 can be extrapolated linearly based on k_B and B30.

If repeated B-readings are not available, k_B can be approximated based on the DMT-RA testing procedure (see green line between A0 and B30 in Figure 2). It was shown by Oberhollenzer et al. (2023) that k_B ranges between $k_B \approx 1 \cdot k_A$ and $k_B \approx 2 \cdot k_A$ in postglacial, Alpine deposits. However, the trend is approximated best by $k_B = 1.5 \cdot k_A$. Again, B0 can be determined based on k_B (derived from k_A) and B30.

A third approach was elaborated to roughly estimate A0 and B0 based on DMT-STD. The percentage decrease of A within the first 15 seconds after penetration stop (d_A) is determined based on the material index (I_D, calculated from A15 and B30) (Oberhollenzer et al. 2023). Since the correlation between d_A and I_D is further influenced by the soil heterogeneity - here defined as the change in soil permeability between two consecutive testing depths - two equations (see Eq. (10) and Eq. (11)) were defined empirically based on DMT-RA to approximate the relation between d_A and I_D. If the difference in I_D between two consecutive testing depths is smaller than 80% it is suggested to use Eq. (9), while d_A is derived from Eq. (10) in more heterogeneous soil layers (leading to a difference in I_D between two consecutive testing depths larger than 80%). As described more detail in Oberhollenzer et al. (2023), A0 can be derived from d_A and is further used in combination with A15 to calculate k_A. k_B should be approximated based on $1.5 \cdot k_A$ and used with B30 to determine B0.

$$d_{A\,homo} = -0.012 \cdot I_D^4 + 0.514 \cdot I_D^3 - 3.495 \cdot I_D^2 + 4.619 \cdot I_D + 7.616 \tag{10}$$

$$d_{A\,hetero} = -1.504 \cdot I_D^4 + 18.11 \cdot I_D^3 - 72.02 \cdot I_D^2 + 93.4 \cdot I_D + 4.42 \tag{11}$$

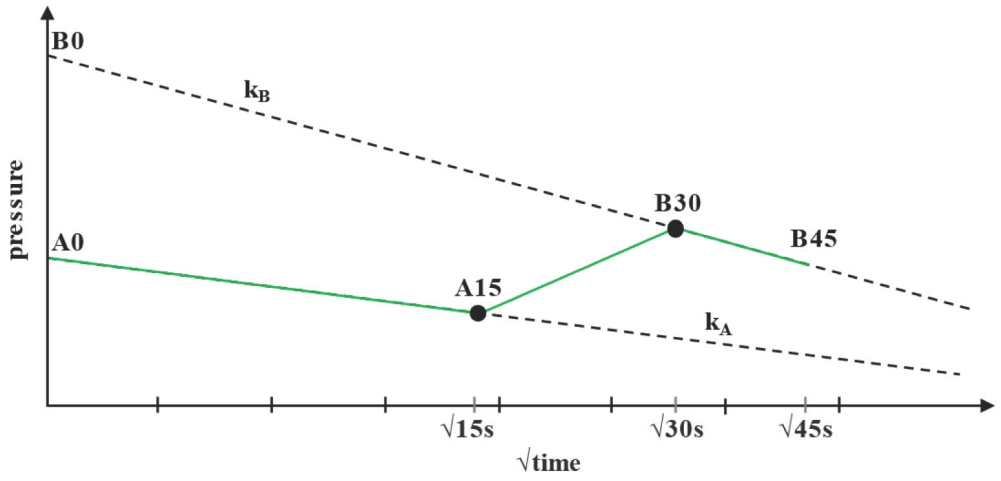

Figure 2. Schematic decrease of DMT readings with the root of time after penetration stop.

2.4 *Soil sampling and laboratory testing*

Soil specimens were recovered by means of tube sampling (*Rhesi*, *Lokalbahn Salzburg*, *water reservoir Raggal*) and block sampling (*Seekirchen*). Sections of highest sample quality were identified based on computer tomography (CT) scans and further used for laboratory testing at Graz University of Technology. Incremental load oedometer tests (IL) and constant rate strain (CRS) oedometer tests were executed on sampled and reconstituted soil specimens according to ISO 17892-5 and ASTM D4186-06, respectively. The soil specimens were loaded from 10 to 960 kPa. Two load steps were considered close to the estimated in-situ effective vertical stress to derive the in-situ constrained modulus (M) (Oberhollenzer 2022).

3 RESULTS

3.1 *Characterization of test sites*

The ground conditions at the test sites *Rhesi*, *Lokalbahn Salzburg*, *Seekirchen* and *water reservoir Raggal* are described based on DMT-STD. The corrected pressure readings (p_0, p_1, p_2), the in-situ pore pressure (u_0) and intermediate parameters (I_D, K_D, E_D, U_D) are shown for individual test sites in Figure 3. In-situ and laboratory investigations are described in more detail in Oberhollenzer (2022).

Test site *Rhesi*, situated in the southeast of lake Constance (47° 28 0 38.4924" N/9° 40 0 5.4912" E), is composed of three main lithologies (L), namely *L1 silty sand* (0 – 2 m), *L2 sand-silt alternations* (2 – 13 m) and *L3 silty clay* (13 – 25 m). The boundaries between individual layers are indicated by grey, dotted lines in Figure 3 (a-e). The top layer (L1), classified as silt (ML) to silty sand (SM) according to ASTM D2487-17e1, is characterized by a strong variation in I_D (= 0.2-2), K_D (= 5-10) and E_D (= 1.5-14 MPa). The groundwater table was situated 0.8 m below the ground level during test execution. A significant scatter is observed for I_D, E_D, U_D and soil classification (lean clays (CL) to silty, clayey sands (SC-SM) according to ASTM D2487-17e1) within L2. While sections with increased fines-content present high values for U_D, the reverse trend is observed for I_D and E_D. K_D values of around 2 indicate normally consolidated conditions within L2 and L3. Fine-grained deposits within L3 are classified as CL according to ASTM D2487-17e1 and are characterized by $I_D \approx 0.2$, $E_D < 4$ MPa and $U_D \approx 0.7$ - 0.8 (see Figure 3a-e).

Postglacial deposits were investigated in the city of Salzburg at test site *Lokalbahn Salzburg* (47° 48′ 58.86″ N/13° 2′ 42.26″ E). Three lithologies, namely *L1 sandy gravel* (0 – 3 m), *L2 sand-silt alternations* (3 – 8.5 m) and *L3 silty clay* (8.5 – 25 m) can be identified based on in-situ and laboratory investigations. As predrilling was required to not damage the membrane, no DMT-STD results are available within L1, classified as silty gravel with sand (GM) based on ASTM D2487-17e1 (see Figure 3f-j). The groundwater table was situated 1.5 m below the ground surface during test execution. Sand-silt alternations (L2) are characterized by a significant scatter of I_D (= 0.3–4), K_D (= 1.5–8), E_D (= 2.5–25 MPa) and U_D (= 0–0.5) in Figure 3 (f-j). Soil classifications according to ASTM D2487-17e1 show a clear scatter within L2, ranging from CL to SC. Small material indices ($I_D < 0.2$) and dilatometer moduli ($E_D < 4$) in combination with large pore pressure indices ($U_D \approx 0.6 – 0.8$) were obtained within fine-grained, lacustrine sediments of lithology L3 (CL according to ASTM D2487-17e1).

Test site *Seekirchen* is situated about 2 km south-west of lake Wallersee (47° 53′ 27.26″ N/13° 7′ 29.73″ E) and can be subdivided into three lithologies: *L1 silty sand* (0 – 3m), *L2 clay* (3 – 12 m) and *L3 moraine* (12 – 13 m). Alluvial sediments of L1 are heterogeneous with respect to the particle size distribution and lead to a pronounced scatter of DMT-intermediate parameters in Figure 3 (k-n) ($I_D = 0.04 – 1.5$; $K_D = 6 – 15$; $E_D = 0.5 – 14$ MPa). No U_D results are shown in Figure 3 (o) as p_2 was not measured. While I_D and E_D are smaller than 0.1 and 1.5 MPa within L2, respectively, K_D decrease slightly over depth but remains larger than 3. The groundwater table was situated 0.8 m below the ground surface during test execution. Soil specimens - recovered within L2 - were classified as fat clay (CH) according to ASTM D2487-17e1.

Young sediments, characterized by an age smaller than 50 years, were investigated within the *water reservoir Raggal* (47° 13′ 11.99" N/9° 50′ 27.83″ E). In-situ testing and soil sampling were executed from a barge to characterize the sedimentation history within the reservoir (Oberhollenzer et al. 2022). Sand-silt alternations of lithology L1 lead to an erratic distribution of DMT-intermediate parameters ($I_D = 0.4 – 5$, $K_D = 0.5 – 6$, $E_D = 0.5 – 12$ MPa and $U_D = 0 – 0.65$) in Figure 3 (p-t). Fine-grained sections characterized by $I_D < 1.2$ are classified as organic silts (OL, OH) according to ASTM D2487-17e1.

3.2 *Determination of in-situ constrained modulus using DMT*

Constrained moduli (M) derived from oedometer tests at the estimated in-situ vertical stress are compared with DMT results at the depth of soil sampling. In the first step, the proposed correlation for clays ($I_D < 0.6$, see Eq. (9)) is evaluated based on laboratory results for the test sites *Rhesi*, *Lokalbahn Salzburg*, *Seekirchen* and *water reservoir Raggal*.

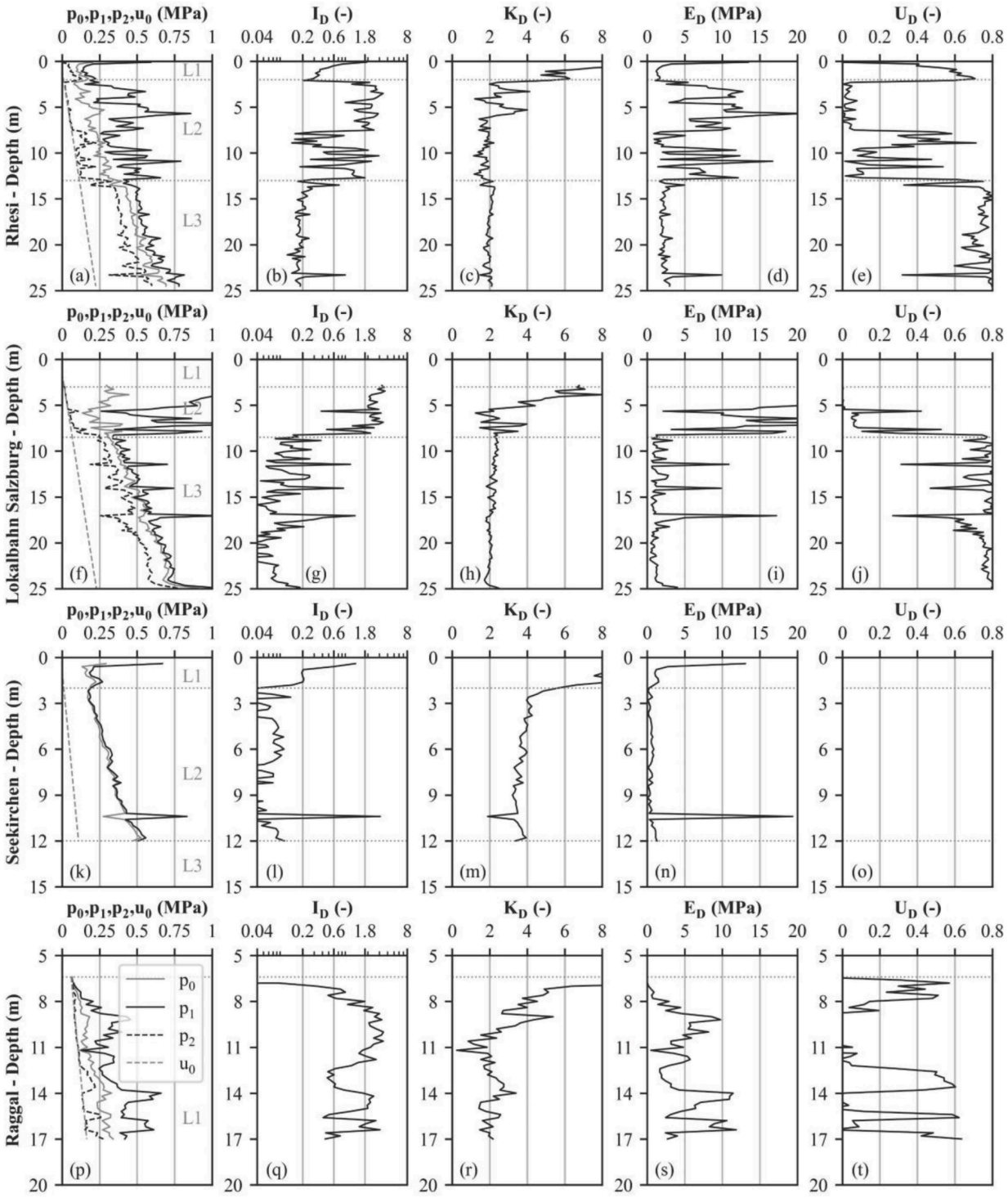

Figure 3. Overview of corrected pressure-readings, in-situ pore water pressure and intermediate parameters at test sites (a-e) Rhesi, (f-j) Lokalbahn Salzburg, (k-o) Seekirchen and (p-t) water reservoir Raggal (the legend for the subplots (a), (f), (k) and (p) is given in Figure 3p).

The constrained modulus (M) derived from oedometer tests, and the dilatometer modulus (E_D) determined at the depth of soil sampling using uncorrected readings (A15, B30) were used according to Eq. (8) to calculate R_M, required to meet the oedometer results (M). The latter R_M values - further declared as $R_{M,required}$ - are compared to I_D and K_D in Figure 4. While individual test sites are indicated by different colors (blue = *Rhesi*, red = *Lokalbahn Salzburg*, green = *Seekirchen* and black = *water reservoir Raggal*), symbols are used to distinguish between different oedometer testing procedures (see legend of Figure 4). The proposed correlation for deriving R_M in clays (Marchetti, 1980) is indicated by a dashed, grey line in Figure 4a. It is shown that the latter correlation leads to

poor agreement with oedometer results and no clear trend can be derived between K_D and $R_{M,required}$ when using uncorrected DMT readings (A15/B30). A better correlation between oedometer and in-situ results can be observed when comparing $R_{M,required}$ and I_D (see Figure 4b). While the upper and lower bounds of this trend are indicated by grey, dotted lines, the best-fit trend is indicated by a grey, dashed-dotted line. The corresponding (best-fit) function is given by Eq. (12).

$$R_M = 0.6 \cdot I_D^{-0.8} \tag{12}$$

In the second step, DMT-readings corrected about partial drainage (A0/B0) are used in combination with oedometer results to derive $R_{M,required}$ (see Eq. (8)). The latter parameter is compared to I_D and K_D - both calculated based on A0/B0 – in Figure 5.

The data points show a smaller scatter if DMT-readings are corrected about partial drainage. However, the proposed correlation by Marchetti (1980) is still in poor agreement with oedometer results (see Figure 5a). A better trend can be derived between laboratory and in-situ results when using the material index I_D (see Figure 5b). Eq. (13) defines the best-fit trend line which is indicated by a grey, dashed-dotted line in Figure 5b. The upper and lower bounds of the trend line are shown by grey, dotted lines in Figure 5b.

$$R_M = 0.3 \cdot I_D^{-1.1} \tag{13}$$

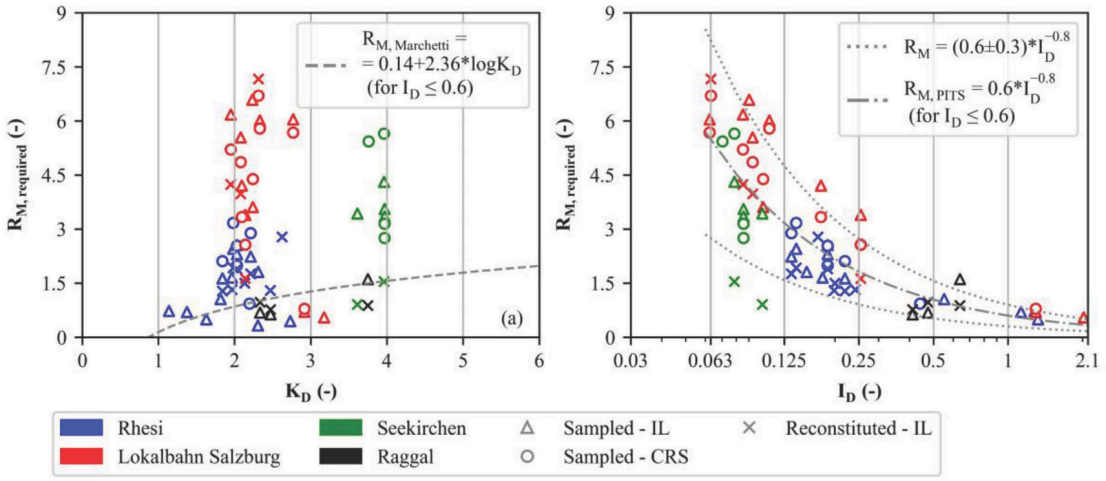

Figure 4. Determination of constrained modulus based on standard DMT-readings (A15/B30): (a) R_M against K_D, (b) R_M against I_D.

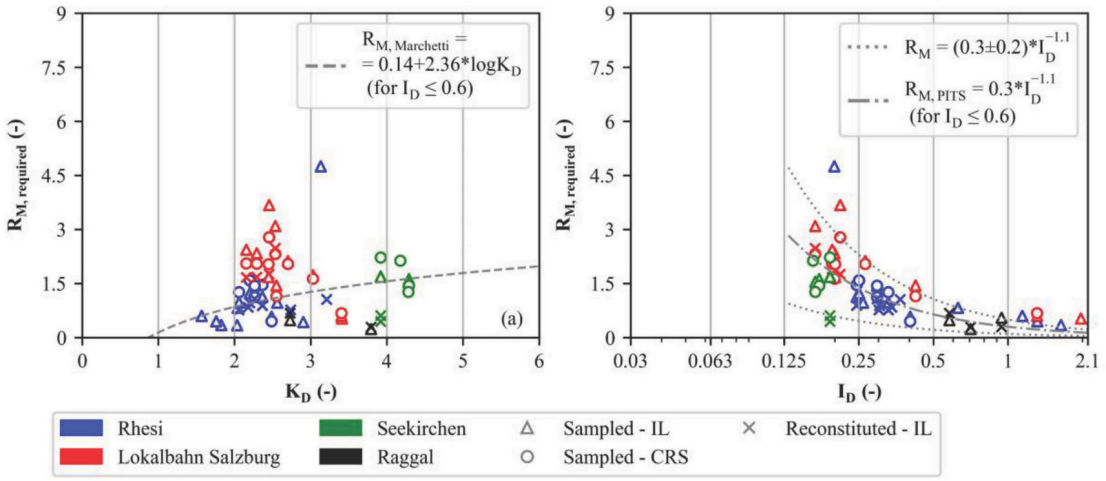

Figure 5. Determination of constrained modulus based on corrected DMT-readings (A0/B0): (a) R_M against K_D, (b) R_M against I_D.

4 CONCLUSION

In-situ and laboratory tests were executed at four test sites (namely *Rhesi*, *Lokalbahn Salzburg*, *Seekrichen* and *water reservoir Raggal*) within the Alpine region to improve the characterization of postglacial, fine-grained sediments. This article aims to improve the determination of the in-situ constrained modulus (M) using the Medusa flat dilatometer test (DMT). In the first step, high-quality oedometer results were compared to the proposed correlation by Marchetti (1980). Subsequently, new correlations are proposed for the DMT to gain an improved agreement with oedometer tests.

The present results indicate that the correlation proposed by Marchetti (1980) underestimates the in-situ constrained modulus in Alpine sediments, classified as lean to fat clays (ASTM D2487-17e1). The agreement between in-situ and laboratory results can be slightly improved if DMT-readings are corrected about partial drainage. New correlations are elaborated for uncorrected and corrected DMT-readings, leading to a better agreement with oedometer results.

It is recommended to (i) use the revised correlations when deriving the in-situ constrained modulus from DMT in Alpine fine-grained deposits and to (ii) correct DMT-readings about partial drainage effects. The applicability of the revised correlations needs to be validated for other locations based on high-quality laboratory tests.

REFERNCES

ASTM D2487-17e1. 2017. Practice for Classification of Soils for Engineering Purposes (Unified Soil Classification System). *ASTM International*, West Conshohocken, PA.

ASTM D4186-06. 2012. Standard Test Method for One-Dimensional Consolidation Properties of Saturated Cohesive Soils Using Controlled-Strain Loading. *ASTM International*, West Conshohocken, PA.

ISO 22476-1. 2012. Geotechnical investigation and testing — Field testing — Part 1: Electrical cone and piezocone penetration test. *International Organization for Standardization*, Geneva.

ISO 22476-11. 2017. Geotechnical Investigation and Testing — Field Testing — Part 11: Flat Dilatometer Test. *International Organization for Standardization*, Geneva.

ISO 17892-5. 2017. Geotechnical investigation and testing — Laboratory testing of soil — Part 5: Incremental loading oedometer test. *International Organization for Standardization*, Geneva.

Marchetti, S. 1980. In Situ Tests by Flat Dilatometer. *Journal of the Geotechnical Engineering Division* 106, GT3: 299–321.

Marchetti, S., Monaco P., Totani G. & Calabrese M. 2001. The flat dilatometer test (DMT) In Soil Investigations -a Report by the ISSMGE Committee TC16." In *2nd International Conference on the Flat Dilatometer*, 7–48.

Marchetti, S. & Monaco P. 2018. Recent Improvements in the Use, Interpretation, and Applications of DMT and SDMT in Practice. *Geotechnical Testing Journal* 41 (5): 20170386.

Oberhollenzer, S. 2022. Characterization of postglacial, fine-grained sediments by means of in-situ and laboratory testing. *Dissertation*, Institute of Soil Mechanics, Foundation Engineering and Computational Geotechnics, Graz University of Technology.

Oberhollenzer, S., Hauser, L. 2022. Research project PITS – Parameter identification using in-situ tests in silty soils. *Final report*, Institute of Soil Mechanics, Foundation Engineering and Computational Geotechnics, Graz University of Technology.

Oberhollenzer, S., Hauser, H., Brand, F., Marte, R. & Schweiger, H.F. 2022. Characterization of young sediments using CPTu and Medusa SDMT. In *Cone Penetration Testing 2022 (CPT22)*: 617–622.

Oberhollenzer, S., Hauser, H., Brand, F., Marte, R., Tschuchnigg, F., Schweiger, H.F. & Marchetti, D. 2023. Characterization of Partial Drainage during Medusa Flat Dilatometer Testing. *Geotechnical Testing Journal* 46 (5): 731–750.

Schnaid, F. 2009. In Situ Testing in Geomechanics - the Main Tests. *Taylor & Francis Group*, London.

Schnaid, F., Belloli, M.V.A., Odebrecht, E. & Marchetti, D. 2018. Interpretation of the DMT in Silts." *Geotechnical Testing Journal* 41 (5): 20170374.

van Husen, D. 1979. Verbreitung, Ursachen und Füllung glazial übertiefter Talabschnitte an Beispielen in den Ostalpen. *Eiszeitalter und Gegenwart* 29: 9–22.